

Review on Point Dipole Approximation in Magnetic Force Microscopy

A Project Report Submitted
in Partial Fulfilment of the Requirements
for the Degree of

MASTER OF SCIENCE

by

Akash Jaiswal

(Roll No. PH14MSCST11001)

Supervisor - Dr. J. Mohanty



भारतीय प्रौद्योगिकी संस्थान हैदराबाद
Indian Institute of Technology Hyderabad

to the

DEPARTMENT OF PHYSICS
INDIAN INSTITUTE OF TECHNOLOGY HYDERABAD
HYDERABAD - 502 285, INDIA

Declaration

I declare that this written submission represents review of research articles mentioned in bibliography in my own words, and where others' ideas or words have been included, I have adequately cited and referenced the original sources. I also declare that I have adhered to all principles of academic honesty and integrity and have not misrepresented or fabricated or falsified any idea/data/fact/source in my submission. I understand that any violation of the above will be a cause for disciplinary action by the Institute and can also evoke penal action from the sources that have thus not been properly cited, or from whom proper permission has not been taken when needed.

Akash Jaiswal

(Signature)

AKASH JAISWAL

(Akash Jaiswal)

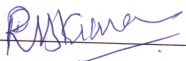
PH14MSCST11001

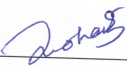
(Roll No)

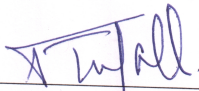
Approval Sheet

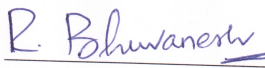
This thesis entitled **Review on Point Dipole Approximation in Magnetic Force Microscopy** by **Akash Jaiswal** is approved for the degree of **Master of Science** from **IIT Hyderabad**.


Examiner


Examiner


Dr. J. Mohanty
Adviser


Examiner


Examiner

ACKNOWLEDGEMENT

The work done in this thesis is a review work on the research papers mentioned in the bibliography of this thesis.

I would like to thank Sachin Grover(M.Sc Student), Diamond Raj Oraon(M.Sc Student) for helping me understand the mathematical concepts involved with this thesis.

I would like to express my deep sense of gratitude to my Parents, God and Family members for their encouragement and support throughout, which always inspired me.

Contents

Declaration	i
Approval Sheet	ii
Acknowledgements	iii
1 Point Dipole Approximation	1
1.1 Model Fields	4
2 Optimization of lateral resolution in magnetic force microscopy	6
2.1 MFM transfer functions	6
2.2 Resolution in magnetic force microscopy	7
2.3 Optimizing conditions	7
2.3.1 The tip	7
2.3.2 Optimum cone angle	9

Abstract

Image interpretation in magnetic force microscopy (MFM) requires details information about the internal microstructure the ferromagnetic tip used for probing the surface microfield of a sample. Since these information are generally not experimentally available, image interpretation is more speculative than rigorously quantitative at the present time. This theoretical analysis confirms by a simple criterion that MFM image interpretation can be perform in terms of point dipole probing provided that some experiment constraints are satisfied. The validity of the criterion is demonstrated for various experimentally relevant example. Starting from tip transfer function (TTF), a minimum detectable wavelength will be used as a measure for the lateral resolution of the instrument. This minimum detectable wavelength will determine the detector noise level in the instrument's configuration.

The model of the minimum detectable wavelength is then used to optimize the tip-sample configuration geometrically as well as magnetically.

Chapter 1

Point Dipole Approximation

Magnetic force microscopy images the local magnetostatic interaction forces between a sharp ferromagnetic tip and the microfield at the surface of ferromagnetic sample.

Image interpretation is quite complicated because of convolution of the sample microfield with tip magnetization. It is mainly because of long-range magnetostatic interaction. Even if these interactions do not cause any mutual deformations of the initial tip and sample magnetization configurations, the microfield interacts with the whole magnetically active tip volume. Thus, the locally detected interaction generally originates to a certain extent from the environment rather than exclusively from that surface point where the microscope tip is actually located. As a result, the ultimately observed image depends critically on the extent of the magnetically active tip volume.

A direct image interpretation in terms of point dipole probing of the microfield distribution would only be possible if the magnetically active tip area could be approximated by a point dipole. In the following, the validity of this approximation depending on the overall microfield environment is discussed.

The magnetostatic potential $V(\mathbf{r})$ of a tip with the dipole moment $\boldsymbol{\mu}$ under the influence of the local microfield \mathbf{c} is given by

$$V(\mathbf{r}) = -\mu_0 \boldsymbol{\mu} \cdot \mathbf{H}(\mathbf{r}). \quad (1)$$

If the magnetically active tip volume is characterized by a certain domain volume V of field-independent extent which carries the saturation magnetization \mathbf{m} , we find

$$V(\mathbf{r}) = -\mu_0 \int \int \int d^3 \mathbf{r}' \mathbf{m} \cdot \mathbf{H}(\mathbf{r} + \mathbf{r}'), \quad (2)$$

where the integration is extended over the fixed tip domain. Thus, according to eq.(1), $V(\mathbf{r})$ can be attributed to the interaction between the local microfield $\mathbf{H}(\mathbf{r})$ and a field-independent dipole moment $\boldsymbol{\mu}(\mathbf{H})$, given by

$$\mu_\alpha(H_\alpha(\mathbf{r})) = \frac{m_\alpha}{H_\alpha(\mathbf{r})} \int \int \int d^3 \mathbf{r}' H_\alpha(\mathbf{r} + \mathbf{r}'), \quad (3)$$

and $\alpha = x, y, z$.

Now, we consider the arbitrary tip domain. The geometrical center of the domain should be located at \mathbf{r} with respect to the surface point under consideration. the three dimensional taylor expansion of the microfield component $H_i(\mathbf{r} + \mathbf{r}')$ around the tip center \mathbf{r} yields

$$\mathbf{H}_\alpha(\mathbf{r} + \mathbf{r}') = \exp(\mathbf{r}' \cdot \nabla) H_\alpha(\mathbf{r}). \quad (4)$$

The corresponding component of tip magnetic moment from eq.(3) is given by

$$\mu_\alpha(H_\alpha(\mathbf{r})) = m_\alpha V + \frac{m_\alpha}{H_\alpha(\mathbf{r})} \sum_{n=1}^{\infty} \sum_{i+j+k=n} \frac{1}{i!j!k!} \times \left(\int \int \int d^3\mathbf{r}' x'^i y'^j z'^k \right) \left(\frac{\partial^i}{\partial x^i} \frac{\partial^j}{\partial y^j} \frac{\partial^k}{\partial z^k} \right) H_\alpha(\mathbf{r}).$$

The first term in the above expression characterizes a component of geometric dipole moment ($\mathbf{m}V$) of the tip with domain volume V . Furthermore since the Taylor approximation is performed with respect to the center of the tip domain, all term of this taylor expansion with odd number in i, j or k vanish completely.

$$\mu_\alpha(H_\alpha(\mathbf{r})) = m_\alpha V + \frac{m_\alpha}{2H_\alpha(\mathbf{r})} \sum_{\eta=x,y,z} \left(\int \int \int d^3\mathbf{r}' \eta'^2 \right) \frac{\partial^2 H_\alpha}{\partial \eta^2}(\mathbf{r}) + \dots \quad (6)$$

Now, the point dipole approximation of the tip, i.e., $\boldsymbol{\mu} = \mathbf{m}V$, is constrained by the criterion

$$\left| \frac{1}{2VH_\alpha(\mathbf{r})} \sum_{\eta=x,y,z} \left(\int \int \int d^3\mathbf{r}' \eta'^2 \right) \frac{\partial^2 H_\alpha}{\partial \eta^2}(\mathbf{r}) \right| \ll 1, \quad (7)$$

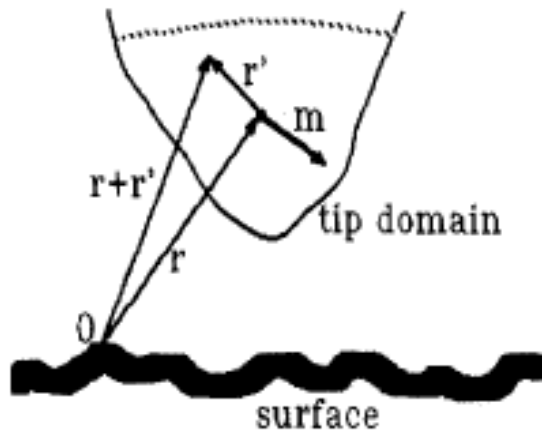


Figure 1.1: Arbitrary shaped tip domain of homogeneous magnetization \mathbf{m} .

The validity of above relation depends on the one hand upon the field and upon its inhomogeneity in the center of the probe, and on the other hand upon the magnetically

active tip volume.

For the simplification of eq.(7) we make some minimum assumptions concerning the typical geometry of experimentally used MFM tips. The obtained tips are generally rather good approximated by a symmetrical cone of length l and angle of aperture θ as shown in below figure. If we perform the integration in eq.(7) for this conical tip model, the point dipole criterion simplifies to

$$\left| \frac{3}{10} \frac{l^2}{H_\alpha(\mathbf{r})} \left[\frac{1}{4} \tan^2\left(\frac{\theta}{2}\right) \left(\frac{\partial^2 H_\alpha}{\partial x^2}(\mathbf{r}) + \frac{\partial^2 H_\alpha}{\partial y^2}(\mathbf{r}) \right) + \frac{\partial^2 H_\alpha}{\partial z^2}(\mathbf{r}) \right] \right| \ll 1. \quad (8)$$

where $\mathbf{r} = (x, y, z)$ defines the geometrical center of the tip.

In the next step of simplification we perform an upper estimation in eq.(8). Let us assume

$$H_\alpha(\mathbf{r}) = H_{0\alpha} \exp\left(\sum_{\eta=x,y,z} \pm \frac{\eta}{\zeta_{\alpha\eta}}\right). \quad (9)$$

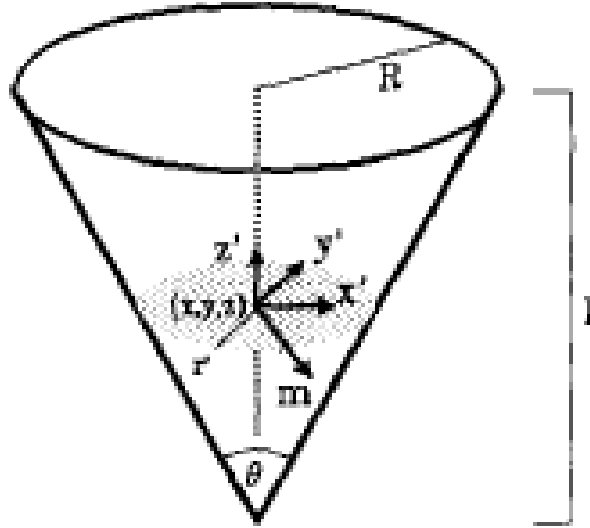


Figure 1.2: Conical tip model of length l , angle of aperture θ and homogeneous magnetization \mathbf{m} .

Then we have

$$\frac{1}{H_\alpha(\mathbf{r})} \frac{\partial^2 H_\alpha}{\partial \eta^2}(\mathbf{r}) = \frac{1}{\zeta_{\alpha\eta}}. \quad (10)$$

Thus, eq.(8) yields

$$\frac{3}{10} l^2 \left[\frac{1}{4} \tan^2\left(\frac{\theta}{2}\right) \left(\frac{1}{\zeta_{\alpha x}^2} + \frac{1}{\zeta_{\alpha y}^2} \right) + \frac{1}{\zeta_{\alpha z}^2} \right] \ll 1, \quad (11)$$

Now for any given field component $H_\alpha(\mathbf{r})$, we constrain the characteristic decay length $\zeta_{\alpha\eta}$ to

$$\frac{1}{\zeta_{\alpha\eta}^2} \gg \left| \frac{1}{H_\alpha(\mathbf{r})} \frac{\partial^2 H_\alpha(\mathbf{r})}{\partial \eta^2} \right|, \quad (12)$$

The performed simplifications of the general formula, eq.(7), now permit an experimentally relevant formulation of the point dipole criterion. For a given field distribution $\mathbf{H}(\mathbf{r})$, MFM images can be simply interpreted in terms of point dipole if eqs.(11) and (12) are simultaneously satisfied for all field components. A useful check of the point dipole criteria is the calculation of these deviations for some selected model fields. For simplicity, we restrict the following model calculations to the one-dimensional case i.e, $H_y = H_z = 0$ and $\frac{\partial^2 H_x}{\partial y^2} = \frac{\partial^2 H_x}{\partial z^2} = 0$ in eq.(11). As a sensitive measure to probe-induced modifications of the field variation we take changes in the $\frac{1}{e}$ -width of two different test fields H_1 and H_2 .

1.1 Model Fields

As first model field we choose

$$H_1 = H_0 \exp\left(-\frac{x^2}{x_0^2}\right), \quad (13)$$

$\frac{1}{e}$ -width of this field is given by decay length x_0 . Now we assume the lateral range of MFM sensing lie between this decay length limit. Then eq.(12) yields for the characteristic decay length

$$\frac{1}{\zeta^2} \geq \frac{2}{x_0^2}. \quad (14)$$

Using $\frac{1}{\zeta^2} = \frac{2}{x_0^2}$ the point dipole criterion, eq.(11), is given by

$$R \ll \left(\frac{20}{3}\right)^{\frac{1}{2}} x_0, \quad (15)$$

with $R = l \tan\left(\frac{\theta}{2}\right)$. As we see that eq.(15) relates the radius R of the conical MFM tip to the decay length x_0 of the field H_1 under investigation. Provided that $R \ll 2.6x_0$, the MFM data should be interpretable in terms of point dipole sensing. The figure below shows the comparison between the probe modified $\frac{1}{e}$ -width of field $\mathbf{V}(\mathbf{r})$ calculated according to eq.(2) and the corresponding value of H_1 in the range $\frac{R}{x_0} \leq 2.6$ according to eq.(15). Thus, the point dipole approximation is satisfactory upto about $\frac{R}{x_0} = 1.5$.

The second model field should be given by

$$H_2 = H_0 \left(1 - \frac{x^2}{x_0^2}\right), \quad (16)$$

The $\frac{1}{e}$ -width is given by decay length $\left(1 - \frac{1}{e}\right)^{\frac{1}{2}} x_0$. If we consider range in this limit for the second model field, the eq.(12) yields

$$\frac{1}{\zeta^2} \geq \frac{2e}{x_0^2}. \quad (17)$$

Taking $\frac{1}{\zeta^2} = \frac{2e}{x_0^2}$, eq.(11) provides the range of validity for the point dipole approximation for H_2

$$R \ll \left(\frac{20}{3e}\right)^{\frac{1}{2}} x_0. \quad (18)$$

Deviations between the $\frac{1}{e}$ -width of $V(\mathbf{r})$ and H_2 are shown in figure. The approximation exhibits a good validity upto about $\frac{R}{x_0} = 1$.

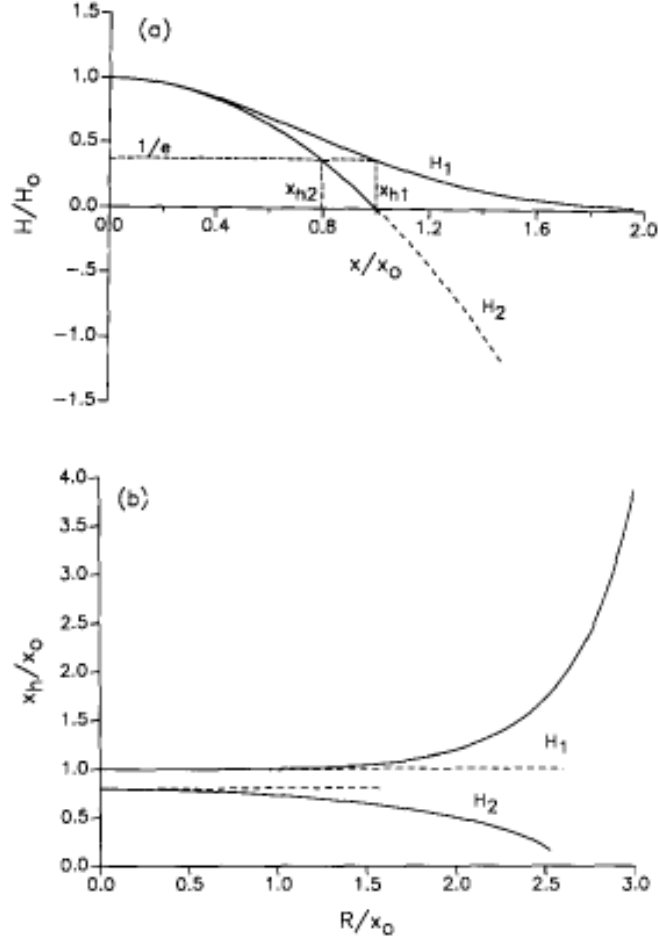


Figure 1.3: (a) The two model fields H_1 and H_2 and their $\frac{1}{e}$ -widths. (b) $\frac{1}{e}$ -widths detected with the MFM for the model fields H_1 and H_2 depending on the radius R of the conical MFM probe (solid lines). The dashed lines illustrate the respective point dipole approximations for the range determined by eq.(15) and eq.(17).

A simple criterion for the point dipole approximation of any given MFM probe is derived. If the criterion is experimentally satisfied, the generally complex interpretation of MFM images become straightforward.

Chapter 2

Optimization of lateral resolution in magnetic force microscopy

2.1 MFM transfer functions

Image formation in an MFM can be seen as a convolution. This kind of problem usually becomes much easier to treat in the Fourier domain. The magnetization pattern $M(x, y, z)$ of a thin film is Fourier transformed in the film (xy) plane only. From the resulting complex $\overline{M}(k_x, k_y, z)$ one can calculate the Fourier transform of the stray field at height z above a sample with thickness h by

$$\begin{pmatrix} \overline{H}_{k_x}(\mathbf{k}, z) \\ \overline{H}_{k_y}(\mathbf{k}, z) \\ \overline{H}_{k_z}(\mathbf{k}, z) \end{pmatrix} = \begin{pmatrix} -\frac{ik_x}{|\mathbf{k}|} \\ -\frac{ik_y}{|\mathbf{k}|} \\ 1 \end{pmatrix} \cdot e^{-|\mathbf{k}|z} \cdot (1 - e^{-|\mathbf{k}|h}) \cdot E_\sigma(\mathbf{k}) \quad (1)$$

where $\mathbf{k} = (k_x, k_y)(m^{-1})$. E_σ can be defined as an effective surface charge which can be calculated for z -independent magnetization structures from :

$$E_\sigma(\mathbf{k}) = -\frac{i}{2} \left(\frac{k_x}{|\mathbf{k}|}, \frac{k_y}{|\mathbf{k}|}, i \right) \cdot \overline{M}(\mathbf{k}) \quad (2)$$

where the dot stands for a vector product. For thin films with perpendicular anisotropy E_σ can be simplified to $E_\sigma = \frac{1}{2M_z}$. Here, the relation \overline{H} and E_σ in (1) will be defined as the field transfer function HTF: $\overline{H} = \text{HTF}E_\sigma$. In magnetic force microscopy, rather than measuring the field, the force on the tip (or its z -derivative) in the z -direction is measured. This is expressed by the force transfer function (FTF), which relates the force on the tip F_z to the stray field ($\overline{F}_z = \text{FTF}\overline{H}_z$). The FTF depends on the shape and the magnetic state of the tip. For a bar-type tip with magnetization M_t , width b , depth S and length Δl it is given by:

$$\overline{F}_z(\mathbf{k}, z) = -\mu_0 M_t b \text{sinc}\left(\frac{1}{2}k_x b\right) \cdot S \text{sinc}\left(\frac{1}{2}k_x S\right) \times (1 - e^{-k\Delta l}) \cdot \overline{H}_z(\mathbf{k}, z) \quad (3)$$

The total transfer from $E_\sigma(\mathbf{k})$ to the force on the tip $F_z(\mathbf{k}, z)$ is then described by the tip transfer function TTF:

$$\overline{F}_{z,\text{magn}}(\mathbf{k}, z) = \text{HTF} \cdot \text{FTF} \cdot E_\sigma(\mathbf{k}) = \text{TTF} \cdot E_\sigma(\mathbf{k}) \quad (4)$$

For the bar type tip this yields:

$$\bar{F}_z(\mathbf{k}, z) = (-\mu_0 M_t) (b \cdot \text{sinc}(\frac{1}{2} k_x b)) (S \cdot \text{sinc}(\frac{1}{2} k_x S)) \times (1 - e^{-|\mathbf{k}| \cdot h}) (1 - e^{-\mathbf{k} \cdot \Delta l}) (e^{-|\mathbf{k}| \cdot z}) E_\sigma(\mathbf{k}) \quad (5)$$

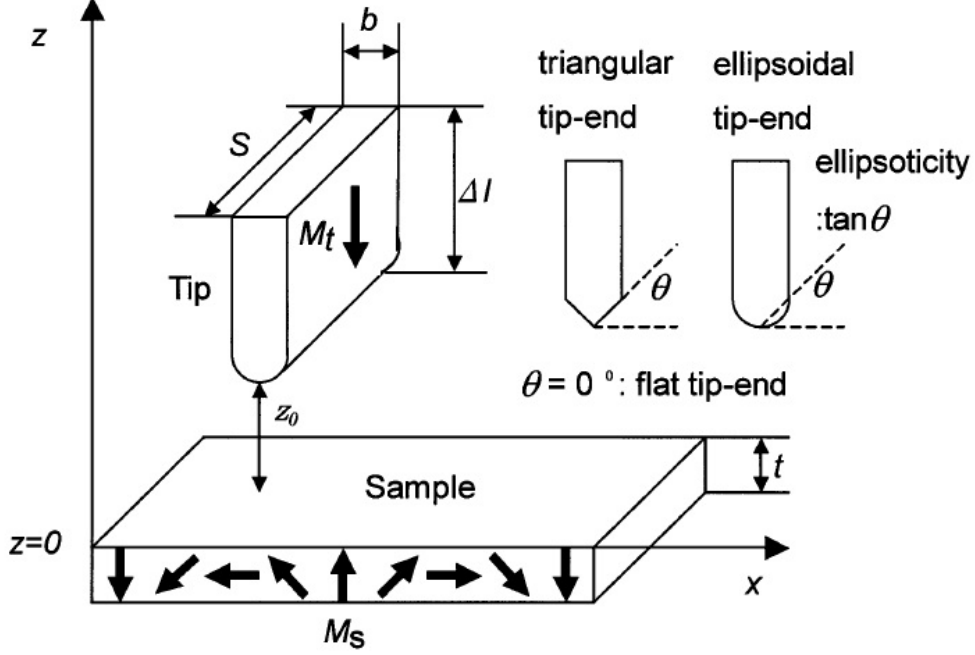


Figure 2.1: MFM model tip.

2.2 Resolution in magnetic force microscopy

Define the lateral spatial resolution of the MFM by the minimum detectable wavelength λ_c , where the TTF drops below the detector sensitivity limit.

In order to flatten the spatial frequency response of the measurement the MFM images can be deconvoluted with the TTF. The λ_c will give the wavelength beyond which mostly noise is amplified, and will still have a meaning.

2.3 Optimizing conditions

λ_c is used to compare different tip-sample configurations and to optimize the measurement conditions for MFM.

2.3.1 The tip

From (3) it is obvious that the tip material must be chosen to have a high magnetic moment in order to get a high signal. For this reason a single-domain tip made from a

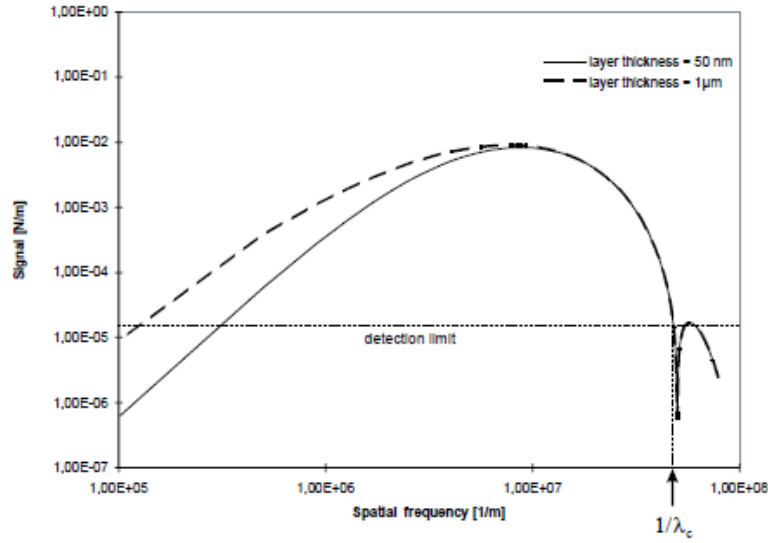


Figure 2.2: k_x direction through the TTF of an MFM using bar-type tip.

material with high M_s will give the highest signal.

Compared with scanning tunneling microscopy, MFM interaction has a longer range. Consequently, larger parts of the magnetic volume of the tip are important. The interaction will not only be determined by the magnetic properties of the tip material but also by the shape of the tip.

The tip's front end dimensions should be as small as possible. This way the integration volume will be small, so that high spatial frequencies can be measured and the tip stray field will have a very rapid decrease in the z -direction, which allows for measurements of soft magnetic materials. This reduces the signal, but with high M_s materials the tip volume can be decreased while still giving enough signal to detect.

Externally applied magnetic fields as well as the sample stray field can change the magnetization of the tip during MFM measurements, which will alter the imaging mechanism during the measurement. A tip switch will be difficult to compensate for if the tip has a hysteresis. To avoid this problem the tip can be made either magnetically very hard, so that it does not change its magnetization during scanning, or very soft, so that it no longer has significant hysteresis.

A very soft tip is always attracted to the sample and will thus image the absolute value of the sample stray field. It loses information about the stray field direction. In order to gain a good signal it must be made from a single domain. Then its switching mechanism must be considered to make it soft. In order to allow free rotation of the magnetization, all shape anisotropy should be excluded, i.e. it must be spherically shaped. For high resolution the volume of these tips must be decreased. Since all three dimensions will have to be reduced by the same amount to keep it a sphere this might drastically decrease the signal for low spatial frequencies. An ideal soft magnetic tip would be a superparamagnetic particle.

A hard tip can measure the polarity of the sample stray field. Since the magnetization of a tip should be as high as possible, the best way to increase its coercivity is to increase

the shape anisotropy rather than to increase the granular structure of the material used. Consequently, a hard magnetic single domain tip should be an elongated needle, which has a high amount of shape anisotropy.

2.3.2 Optimum cone angle

The question is now whether a sharpening of the needle end can improve its performance. In order to find an answer to this question the TTFs have been calculated and compared for different top angles.

The difference in the tip apex angle influences the signal of the tip. For this reason the widths of the tips are adjusted in such a way that they all give the same maximum signal. Figure 2.2 shows the transfer functions of two hard magnetic tips, one having a flat top and one with a top angle of 43° . The width b of both tips has been adjusted in such a way that they both give the same maximum signal ($b = 20\text{nm}$ for the flat top and $b = 73\text{nm}$ for the 43° top). From the figure it can be seen that the flat bar tip has a zero in the transfer function at $\lambda = b$. With increasing tip angle this zero vanishes and the curve becomes flatter. The flat-top tip, however, has the larger signal in the high-resolution region. Since the tip thickness can be scaled in any case, the interesting details of the image can be brought into this region and can be imaged with a higher signal to noise ratio.

For negative tip angles the situation is shown in fig. 2.3. Such type of tip can be design to focus the tip stray field above the sample to improve resolution. The TTF, however, shows many pronounced zeros, which will make this type of tip impracticable.

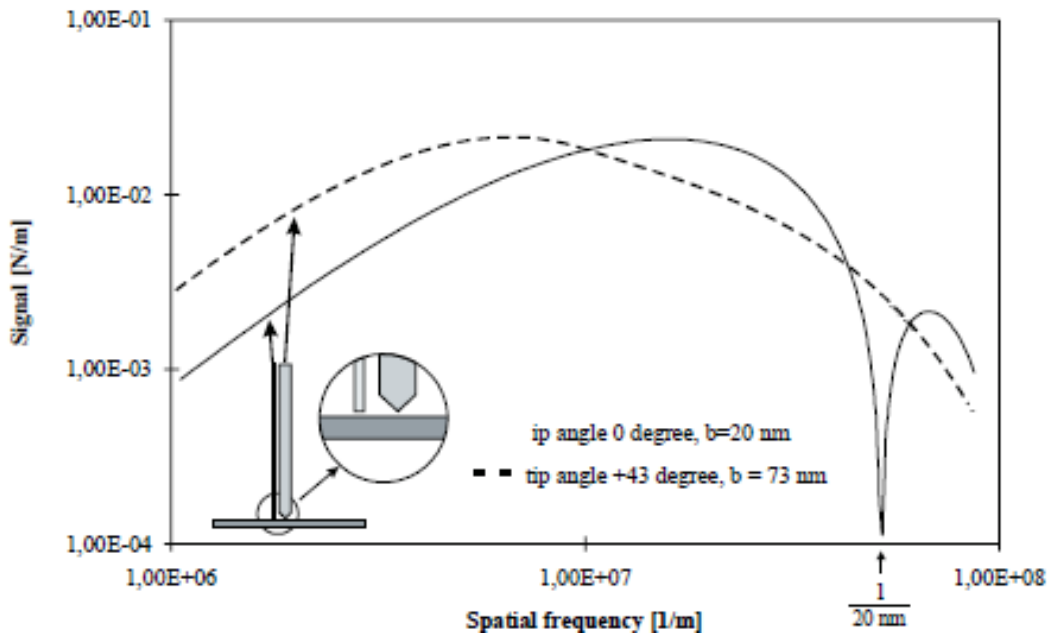


Figure 2.3: Cross-section in the k_x direction through the TTF of a tip with positive cone angle compared with the flat tip.

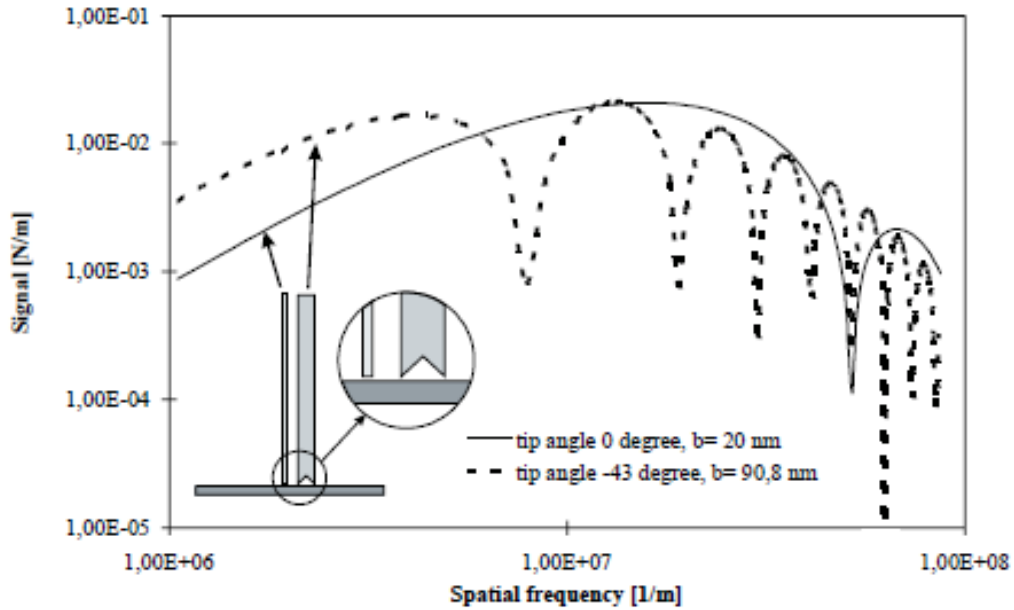


Figure 2.4: Cross-section in the k_x direction through the TTF of a tip with negative cone angle compared with the flat tip.

Conclusions: For image formation in an MFM a tip transfer function (TTF) can be calculated for each tip and sample configuration. From the detection sensitivity a minimum detectable wavelength can be derived which is a measure for the lateral resolution that take place into account both the tip and the sample.

The MFM resolution can be enhanced by reducing the tip front surface. In order to lower the influence of the tip on the sample the tip volume must be reduce rather than the tip remanent magnetization, since in this way the resolution will increase too. So the lateral resolution and the minimum sample coercivity of the magnetic force microscope will not disturb the sample magnetic structure will depend on the sensitivity of the MFM detector and on the ability to fabricate small enough magnetic volume with high remanent magnetization.

Bibliography

- [1] H. J. Hug, B. Stiefel, A. Moser, R. Hofer, P.J.A. Van Schendel, A. Klicznik, H. J. Guntherodt, S. Porthun, L. Ambelmann, J.C. Lodder: in press.
- [2] S. Porthun, L. Abelman, J. C. Lodder: J. Magn. Magn. Mater. in press.
- [3] M. Ruhring, S. Porthun, J. C. Lodder, S. Mcvitie, L. J. Heyderman, A. B. Johnston, J. N. Chapman: J. Appl. Phys. 79, 6(1996).
- [4] U. Hartmann, J. Appl. Phys. Lett.53 (1988) 1561.
- [5] J. J. Saenz, N. Garcia, P. Grutter, E. Meyer, H. Heinzelmann, R. Wiesendanger, L. Rosenthaler, H. R. Hidber and H. J. Guntherodt, J. Appl. Phys 62 (1987) 4293.